First European Conference on Earthquake Engineering and Seismology
(a joint event of the 13th ECEE & 30th General Assembly of the ESC)
Geneva, Switzerland, 3-8 September 2006
Paper Number: 1371

DAMAGE DISTRIBUTION AND SEISMOLOGICAL MODEL OF THE NOVEMBER 2004, SALÒ (NORTHERN ITALY) EARTHQUAKE

Vera PESSINA[1], Gianlorenzo FRANCESCHINA[1], Paola VANNOLI[2], Lucia LUZI[1] and Francesca PACOR[1]

SUMMARY

The West side of lake of Garda, in Northern Italy, was struck by a M_L=5.2 earthquake on November 24, 2004. The felt area is rather large (from Venice to Milan) and the damaged area consists of 66 municipalities, with a number of homeless of about 2200 and estimated direct damages of 215 millions of euros. Most of the damaged structures are old masonry buildings and churches, while there were almost no damage to reinforced concrete structures. The observed distribution of macroseismic intensity shows a strong azimuthal dependence, with high intensity level in a 10x10 km^2 area located SW to the epicentre and rather large dispersion of values (ranging from V to VII-VIII) in the first 10 km epicentral distance.
Taking into account the vulnerability level of the damaged structures and the features of the geological formations, we tried to explain the observed damage distribution in terms of finite fault properties of the source, despite the moderate magnitude of the event.
Thus we hypothesised a fault geometry from seismotectonic considerations and we simulated the event by a high frequency simulation technique (Deterministic Stochastic Method, DSM). The synthetic ground motion parameters were converted into intensity values by empirical relationships and local geological conditions were considered to explain some discrepancies between simulated and observed intensities. It was possible to adequately reproduce both the observed distribution of macroseismic intensity and the ground motion recorded by an accelerometric station located at about 13 km epicentral distance.

1. INTRODUCTION

The November 24, 2004 (23:59 local time) event struck the West side of the Garda Lake (Northern Italy) with a magnitude M_L = 5.2 (M_W = 5.0). Its epicenter was located at 45.685 N and 10.521 E [INGV-CNT Seismic Bulletin], and the depth was estimated at around 10 km [Augliera et al., 2006].
The maximum intensity I_{MCS} = VII - VIII was felt in the municipalities of Vobarno, Salò, Gardone Riviera and Toscolano Maderno [QUEST, 2005], but the total hit municipalities were 66, with felt intensity ranging between V and VII-VIII: 3500 residential buildings, 200 public structures and about 300 churches were damaged; the homeless were about 2200 and the damages were estimated on 215 millions of euro (*http://www.provincia.brescia.it/protezione-civile/terremoto)*
Despite the relative low magnitude, maximum intensities were not symmetrically distributed around the epicentre (Figure 1). A 10x10 km^2 area located SW to the epicentre experienced the highest observed values (ranging between VI and VII-VIII). NE and NW sites located at comparable distances (10-15 km) do not show

[1] Istituto Nazionale di Geofisica e Vulcanologia – Sezione di Milano, via Bassini,15, Milano, Italy.
Email : pessina@ingv.mi.it, glf@ingv.mi.it; luzi@ingv.mi.it, pacor@ingv.mi.it
[2] Istituto Nazionale di Geofisica e Vulcanologia – Sezione di Roma 1. via di Vigna Murata, 605, Roma, Italy.
Email : vannoli@ingv.it

similar levels of damage (being observed MCS intensities V and V-VI, respectively). As a consequence, macroseismic intensities show a large dispersion (ranging from V to VII-VIII) up to 10 km epicentral distance: in Figure 2 the observed values are compared with those estimated by intensity attenuation relationships developed on Italian data [Grandori et al.,1991; Faccioli and Cauzzi, 2005].

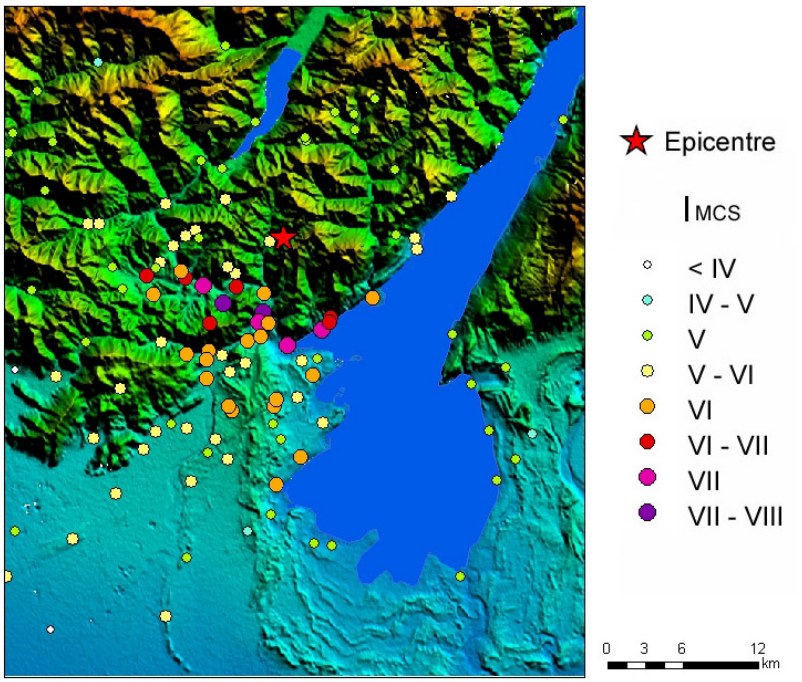

Figure 1: Macroseismic data distribution of the November 24, 2004 earthquake (5.0 M_W)

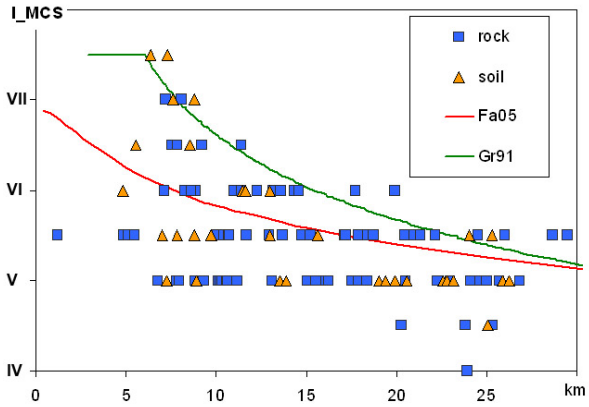

Figure 2: Distribution of the observed intensity with epicentral distance, considering simplified geological characterization. Coloured lines refer to estimated intensity values with Italian attenuation relationships: Fa05 [Faccioli and Cauzzi, 2005], Gr91 [Grandori et al.,1991]

It is noteworthy that localities with maximum observed intensities (I_{MCS} = VII – VIII) are located on soil (see § 3.2) and could be influenced by probable geological amplification effects. However, even considering the paucity of the observations in North-East area, geological effects lonely seem to be inadequate to explain the features of the macroseismic observations in the 5-15 km range, for sites having VI and VI-VII intensity degree (see Figure 2). Taking into account the local heterogeneities (possibly due to geological or geo-morphological site effects) and the vulnerability level of the area [Regione Lombardia e CNR, 1996], we investigate the observed ground shaking anisotropy by considering possible finite fault effects of the source.
Moderate- and low-magnitude earthquakes are generally simulated by point source models. However, in the case of November 24, 2004, Salò (M_L=5.2) earthquake, in order to reproduce the observed damage, we prefer to introduce a finite fault hypothesis based on seismotectonic considerations. An asymptotic simulation technique, the Deterministic-Stochastic Method (DSM) of Pacor et al. [2005], was employed with different kinematic models of the rupture process on the fault. The spectral attenuation model was inferred from estimates of the

quality factor performed with data of local earthquakes recorded in 2003 [Marzorati et al., 2004; Augliera, 2006, personal communication], and high frequency attenuation, generally ascribed to surface propagation, was inferred from acceleration data recorded during the main event at Vallio Terme (13.3 km epicentral distance) [SSN,2005].
Uncertainties affecting the location of the main shock allowed varying the nucleation point position over the assumed fault plane. Ground shaking maps obtained with different hypothesis on the rupture starting point show strong variability, mainly due to the low dip angle hypothesized based on seismotectonic setting. A shape comparison between the simulated distribution of peak ground values and the observed macroseismic data was performed in order to define the best position for the rupture nucleation. A comparison between synthetic and recorded spectra accelerations obtained at Vallio Terme (GVD), classified as "rock site" [Pergalani et al., 2005], allowed to calibrate the most appropriate simulation parameters.
Different empirical relationships were tested to convert the simulated strong motion parameters into macroseismic intensity, and the most suitable was adopted.
A final comparison between the simulated scenario and macroseismic data was performed by taking into account standard vulnerability levels. On the other hand, small-scale (1-2 km) geological heterogeneities have been accounted only for sites with the highest intensity values, in order to quantify possible reduction coefficients.

2. GROUND SHAKING SCENARIOS

2.1 Seismotettonic setting

The studied area is located along the margin of the Southalpine chain, that formed in the framework of the Africa-Europe convergence since the Miocene [e.g. Doglioni and Bosellini, 1987]. Significant uplift has been documented to have occurred since the Pliocene [Zanferrari et al., 1982]. The Garda Lake area is affected by the Giudicarie fault system, related to NNE-SSW trending thrusts and transpressional structures (Figure 3). The activity of these thrusts, with minor oblique component, is consistent with the available data on the present-day kinematics inferred by focal mechanism [Slejko et al., 1989; MEDNET, 2006], minimum horizontal stress from breakouts data [Montone et al., 2004] and GPS measurements [D'Agostino et al., 2005]. The main active structures of the Southalpine sector are usually blind thrusts. Geomorphological and paleoseismological investigations carried out in this area did not identified the major faults responsible for the larger earthquakes [e.g. Galadini et al., 2001].
A significant seismicity affects the southern Garda Lake area (1802, 1222, and 1901 earthquakes), while moderate seismicity affects the northern area and the Mt. Baldo sector, like the 1932, 1882, 1876 earthquakes [Boschi et al., 2000]. In 1046 a strong earthquake, unknown to the Italian seismic catalogues, affected the Mt. Baldo and the valley of the river Adige, where more than thirty castles collapsed [Guidoboni and Comastri, 2005]. The whole earthquakes show an alignment of epicenters along the Giudicarie fault system (Figure 3). In the Database of Individual Seimogenic Sources (DISS) the seismogenic sources responsible for the 1802 and 1901 earthquakes are identified through geological and geophysical investigations [DISS Working Group, 2006].

2.2 Seismogenic source of the November 2004, Salò earthquake

We used a wide spectrum of geological and seismological data, including kinematic and geodynamic constraints, in order to investigate the November 24, 2004 earthquake source. Fault plane definition is based on both main shock and aftershocks hypocenters location estimated at about 10 km and between 10 and 14 km depth, respectively [INGV-CNT Seismic Bulletin; Augliera et al., 2006]. The focal mechanism [MEDNET, 2006] shows the northwest-dipping plane in agreement with the geometry of the thrust of the Giudicarie fault system.
The November 2004, Salò earthquake confirms the mechanism of tectonic deformation in the Southalpine chain, and the style of seismogenic faulting of the Giudicarie fault system region, as previously suggested in the DISS. Consequently, we hypothesized that the 2004 earthquake ruptured a portion of the Giudicarie thrust system located on the same thrust fault of the 1901 earthquake seismogenic source at a larger depth. Length and width of the source have been derived using Wells and Coppersmith [1994] relationships (Table 1).

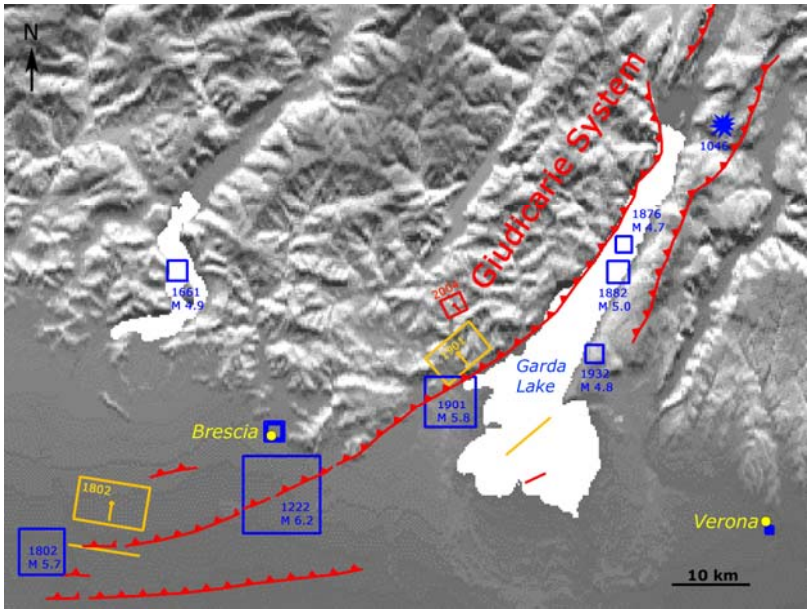

Red hachured line: main thrusts of the *Giudicarie fault system* defined in literature

Red rectangle and red line: surface projection and projected cut-off of the blind fault plane of the 2004 earthquake

Yellow rectangles and yellow lines: surface projections and projected cut-offs of the blind fault planes identified in DISS [DISS Working Group, 2006]

Blue squares: historical earthquakes with date and magnitude [Boschi et al., 2000]

Blue star: epicentral area of the 1046 earthquake [Guidoboni and Comastri, 2005].

Figure 3: Seismotectonic sketch of the studied area. Note the general agreement between the locations of November 24, 2004 and October 30, 1901 events.

Table 1: Geometric and kinematic parameters of the seismogenic source responsible for the 2004 Salò earthquake. Geographical coordinates refer to the eastern upper tip of the fault plane.

Parameter	Value	Derived by
Latitude	45.683	Based on seismological and geological data.
Longitude	10.529	
Length	2.6 km	Calculated using the relationship by Wells and Coppersmith (1994).
Width	2.5 km	
Minimum depth	10.0 km	Based on seismological and geological data.
Maximum depth	11.0 km	Derived from minimum depth, width, and dip.
Strike	246°	Based on MEDNET (2006), and according to geological data
Dip	24°	
Rake	113°	
Average slip	0.3 m	Calculated using the relationship by Kanamori and Anderson (1975).

2.3 DSM simulation

2.3.1 Modelling method

The Deterministic-Stochastic Method of Pacor et al. [2005] is a modification of the stochastic point source simulation method of Boore [2003], accounting for finite fault effects by a simplified formulation of the isochron theory [Bernard and Madariaga, 1984; Spudich and Frazer, 1984]. A kinematic rupture model is introduced by specifying the nucleation point on the fault plane, from which the rupture propagates radially outward with a prescribed rupture velocity, and the final slip distribution. The synthesis of a time series is a four-step procedure consisting of:

I) Computation of the deterministic acceleration envelope of shear waves radiated from an extended fault.
II) Generation of a white noise time-sequence and windowing with the envelope computed in step I).
III) Introduction of the point-source-like reference spectrum. The time sequence obtained in steps II) is transformed into the frequency domain and multiplied with the point-source-like amplitude spectrum

$$A(\omega, R) = \omega^2 \cdot C \cdot G(R) \cdot S(\omega) \cdot A_p(\omega, R) \quad (1)$$

where ω represents the angular frequency and R is the average source-to-site distance, computed through the isochron theory. C is a constant including the free surface amplification factor (Fs = 2), the average radiation pattern for S waves ($R_{\theta\varphi}$ = 0.63), the energy partitioning factor between the two horizontal components of the motion (V=0.707) and the density and S wave velocity at source (ρ=2.8 g/cm^3 and β=3.5 km/s, respectively). G(R) is the geometrical spreading factor, $A_P(\omega, R)$ stands for attenuation model $A_P(\omega,R) = \exp(- \omega R / 2\beta Q(\omega)) \exp(- \omega k / 2)$, specified in terms of quality factor $Q(\omega)$ and diminution parameter k [Anderson and Hough, 1984]. Source term $S(\omega)$ is characterized by a ω–square model described by seismic moment, M_0, and apparent angular corner frequency, ω_a , proportional to the inverse of the apparent rupture duration as perceived by the observer.

IV) Transformation back to the time domain of the complex acceleration Fourier spectrum obtained in step III).

Application of steps from I) to IV) implies that the resulting acceleration time series involves stochastic properties of the adopted Gaussian white noise and deterministic properties of the acceleration envelopes and point-source-like reference spectra (obtained by means of the kinematic finite-fault source modelling) .

2.3.2 Modelling details

Table 1 summarizes the source parameters adopted for simulation of the event. We consider the above described source geometry with different nucleation points located in the deepest half of the fault. A constant rupture velocity of 2.5 km/s and a homogeneous slip distribution is assumed in all simulations. The spectral attenuation model $A_P(\omega,R)$ involves $Q(f) = 58.3\ f^{0.86}$ [Augliera 2006, personal communication], and the high frequency diminution parameter k, estimated using horizontal components recorded at Vallio Terme (Figure 4). A mean value of k=0.04 s was inferred from regression of spectral acceleration data in the range 8-25 Hz, and adopted as representative value of average soil conditions in order to simulate the ground shaking up to 35 km epicentral distance. Simulations were performed at grid points regularly spaced of 2 km and at Vallio Terme (GVD), in order to compare recorded and synthetic data.

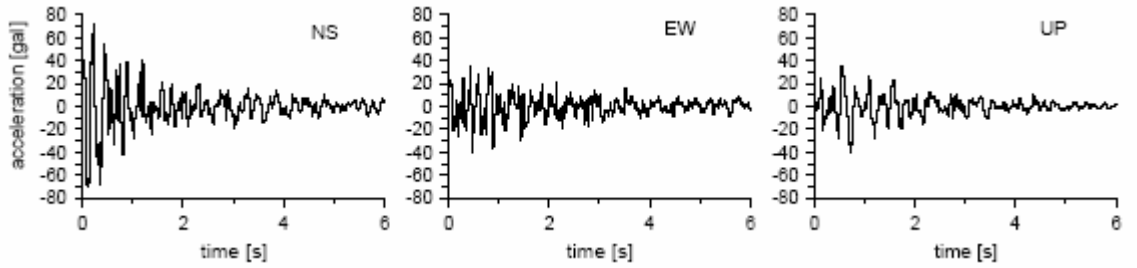

Figure 4: Acceleration data recorded at Vallio Terme (13.3 km epicentral distance) during the November, 24, 2004 Salò earthquake.

2.3.3 Results

Figure 5 shows the a_{max} maps obtained with different rupture models, corresponding to different position of the nucleation point (see top/right panel). Despite the moderate magnitude, the low dip angle involves a high variability in ground shaking with maximum shaking areas located up to 10 km far from the epicentre. A part from small-scale heterogeneities, a qualitative comparison with macroseismic data seems to favour B and D nucleation points. A similar conclusion can be inferred from comparison of synthetic and recorded acceleration data at Vallio Terme (GVD). Figure 6 shows amplitude Fourier spectra of the recorded horizontal components compared with mean horizontal components simulated with different rupture models. Acceleration spectra obtained at GVD are less sensitive to variations of the rupture starting point. However, cases B and D produce the better fit between synthetic and recorded spectra. It is noticeable that nucleation points from A to E produce at station GVD, mean horizontal a_{max} of 47.9, 69.9, 42.9, 105.0 and 210.8 gal, respectively, and recorded a_{max} are 69.6 and 41.0 gal for NS and EW components, respectively.

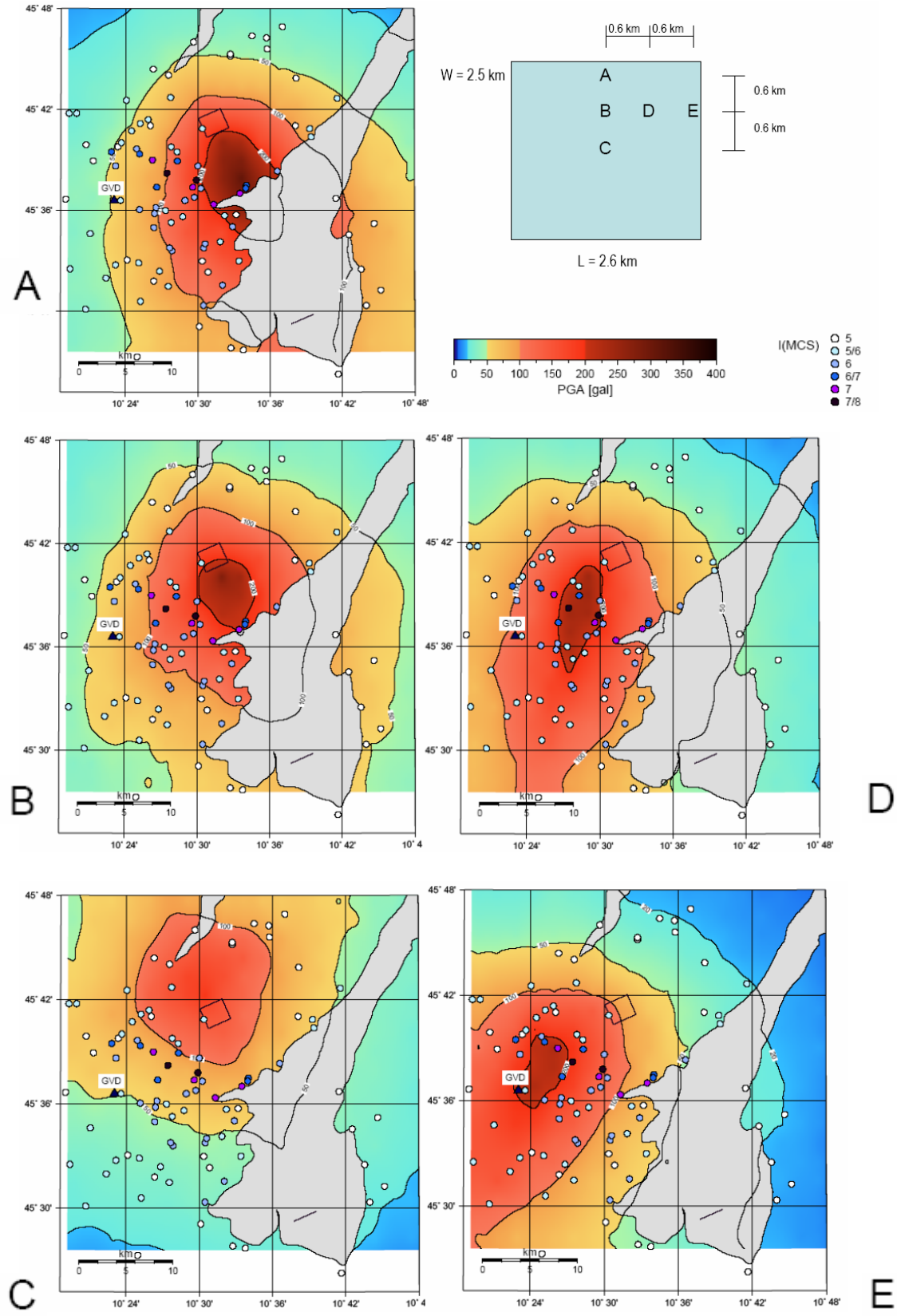

Figure 5: The November 24, 2004 Salò earthquake: synthetic a_{max} obtained by DSM simulations with different rupture scenarios and schematic view of the adopted fault geometry. Hypothesized nucleations points are labelled as A, B, C, D, E on fault and maps. The observed macroseismic intensities (MCS) and the location of Vallio Terme (GVD) are also shown.

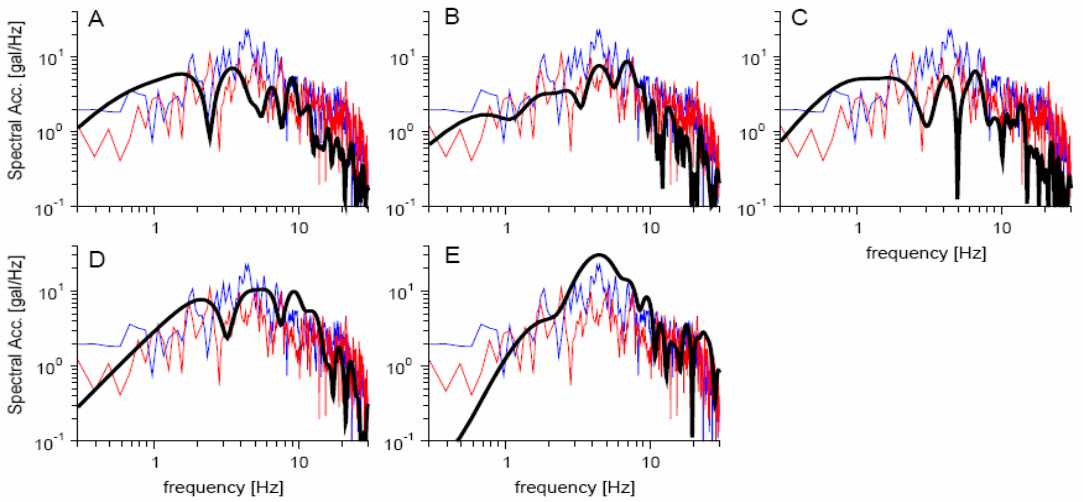

Figure 6: Comparison between DSM synthetic (black line) and recorded (blue line: NS component; red line: EW component) acceleration spectra of the November 24, 2004 Salò earthquake at station GVD.

3. SYNTHETIC AND OBSERVED DAMAGE SCENARIOS

Opportune conversion relationships were used to make the comparison between the intensity distribution estimated from DSM simulations and the observed macroseismic data.
Because of the synthetic simulations were performed for rock conditions, intensity values have to be decreased of the eventual contribution due to local soil effects. Indeed local soil conditions are in general considered able to increase the felt intensity values: according to a systematic analysis of French macroseismic database (Bossu et al, 2000), the probability of observing a site effect on sediment is ranging from 52 % to 83%, while the probability that the intensity increase exceeds one degree ranges from 4% to 26%, according to the age of the soil.

3.1 Ground shaking parameters and their conversion

A first level of analysis makes use of relationships between I_{MCS} and peak ground acceleration (a_{max}) or peak ground velocity (v_{max}). The use of more than one relationships is justified by the awareness of the limits of ground shaking parameters conversion.

Based on Italian macrosesimic dataset, the attenuation of Margottini et al. [1992] provides good results at low intensity values (generally up to VII grade). Its forms is:

$$a_{\max} = 3.353 \cdot 10^{0.220 I} \tag{2}$$

Recently new relations, developed by Faccioli and Cauzzi [2005], were calibrated on the enlarged previous dataset with the purpose to include event with intensity bigger than VIII; they are based on a_{max} and v_{max} parameters, as following:

$$I = 1.83 \cdot \log a_{\max}\left[m/s^2\right] + 6.57 \tag{3}$$

$$I = 1.65 \cdot \log v_{\max}\left[m/s\right] + 8.52 \tag{4}$$

The last relationship adopted in this work is calibrated on historical damage observations and acceleration records of the 1976 Friuli event [Rebez and Slejko, 2004] and it is appositely developed for North-East Italy, assuming a basic equivalence of the EMS98 and MCS scale in the IV to VIII range:

$$I = 2.10 + 4.35 \cdot \log a_{\max}\left[g \cdot 100\right] \tag{5}$$

Fig. 7 shows, for comparison, the differences between the recorded and the estimated intensity values, respect to epicentral distance (on the right) and azimuth (measured clockwise from strike direction) (on the left). Eq. (2) and (5) show almost the same behaviour, as well as Eq. (3) and (4). However, the last two relationships show a lower scatter of data and a higher prediction capability at large distances. For this reason, we adopted the relationships (3) and (4) in our analysis.

We simulated the November 24, 2004 Salò earthquake by DSM, considering the rupture model D and performing simulations at 136 sparse sites corresponding to macroseismic observations points. Simulated a_{max} and v_{max} were converted into macroseismic intensities by Eq.(3) and (4), respectively. Figure 8 shows observed and synthetic intensities versus azimuth (measured clockwise from strike). Both intensities based on a_{max} and v_{max} follow the observed intensity distribution, with maximum values in the range 90-200°. It is noteworthy that the maximum variability is obtained at about 140°, where observation points span an epicentral distance interval ranging from 5 to 30 km. In this direction (corresponding to SW), maximum values of intensities are located between 5 to 10 km epicentral distance. In the opposite direction (320°), simulated intensities refer to the same range of epicentral distances (5 – 10 km), and they are at least 1 degree lower than maximum intensities obtained at 140° azimuth. In the NE (320°) case, however, simulated intensities tend to overestimate the observed ones of about 0.5 degree. Moreover, in the first 100 km, differences between observed and predicted intensities (I_{MCS}-I_{est}) calculated by v_{max} (eq. (4)) and a_{max} (eq. (3)) are (-0.51 ± 0.53) and (-0.73 ± 0.62), respectively.

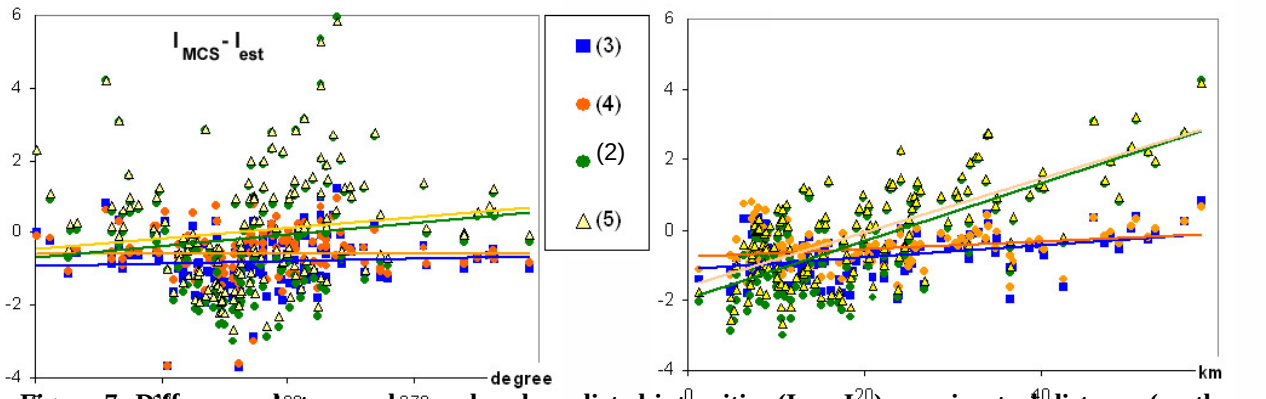

Figure 7: Differences between observed and predicted intensities (I_{MCS}-I_{est}) vs epicentral distance (on the right) and azimuth (left): coloured dots refer to equations (2) (3) (4) and (5); coloured lines are corresponding linear regressions.

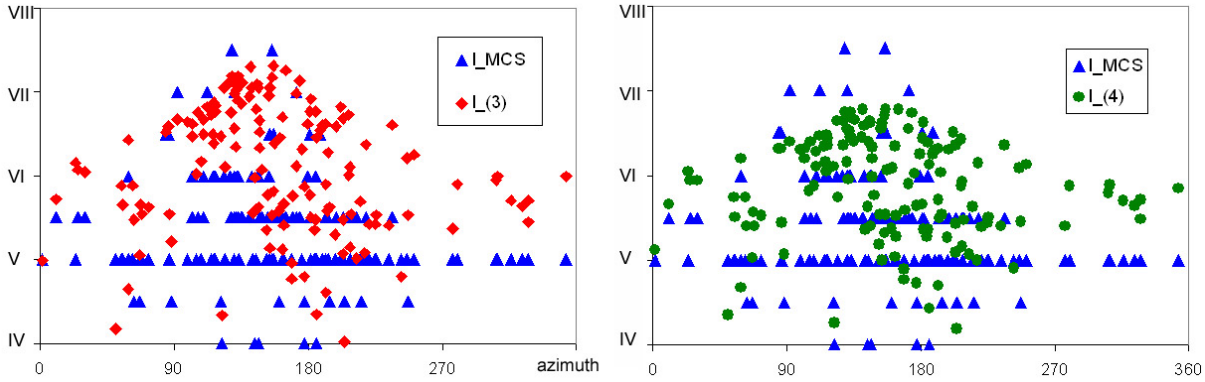

Figure 8: Observed and synthetic macroseismic intensities, vs azimuth. Red dots: synthetic intensities obtained by DSM simulations (a_{max} from scenario D) and equation (3); Green dots: synthetic intensities obtained by DSM simulations (v_{max} from scenario D) and equation (4); Blue dots: observed intensities.

3.2 Vulnerability and geological site effects

The vulnerability level of most of the involved municipalities is know because of a detailed survey previously carried out with seismic purposes by Regione Lombardia and CNR [1996]. The vulnerability level of the localities with the highest intensity is illustrated in Table 2, grouped into three classes (A = low, B = medium and C = high). Vulnerability values are in agreement with the assessments made at national scale [Bernardini, 2000] using the Italian National Institute of Statistic data [ISTAT, 1991] based on a national-wide census of dwellings. Evidence of particular high level of vulnerability was detected in the historical centres, otherwise a general good quality of the residential structures can be assumed. In the present work, we did not adopted corrective vulnerability factors and we considered homogeneous moderate vulnerability, at least at municipal scale.

Table 2: Vulnerability characterization and geological setting of the localities with maximum intensity

#	Municipality-Localitity	I_{MCS}	Ground condition	Vul. level	Note
1	Sabbio Chiese - Cibbio	VII-VIII	soil		not classified
2	Vobarno - Pompegnino	VII-VIII	soil		not classified. Indicative municipality's value: *medium*, moderate quality data.
3	Gardone Riviera - Morgnaga	VII	rock	B, C	moderate quality data
4	Sabbio Chiese - Pavone	VII	soil	A	moderate quality data
5	Roè Volciano	VII	rock	A, B, C	moderate quality data, high vulnerability in historical centres
6	Salò	VII	soil	A, B	low quality data, partial classification

The geological setting of each localities was checked on a 1:100.000 geological map: two main classes (rock and soil) were defined by the features of the surface characteristics (age and type of deposits). Figure 2 shows the distribution of intensity observations with distance considering the geological classification: analysis are limited in the first 30 km because all the farthest localities are located on soil, in the Pianura Padania.
The sites #1 and #2 with I = VII-VIII (see Table 2) are located on fluvioglacial deposits and they have been investigated for probable amplification effects: the time series of the deterministic simulation were used as input in a simplified 1D analysis [EERA code, Bardet et al., 2000]. The amplification factors (value on soil/on rock) vary in the ranges (1.2 – 1.6) and (1.6 – 2.3) in terms of a_{max}, and v_{max} respectively.
Converting the ground motion amplification in terms of intensity, using the (4) relationship, the increment of intensity is ranging between 0.4 and 0.59: in this case we can assume that, if amplification effects occur, they could be quantified in a half degree increment, in agreement with commonly used operative indications [Bard, 1998].

4. CONCLUSIONS

By comparison between synthetic scenarios and macroseismic data, we can confirm that the resulting pattern of synthetic intensity shows a good agreement with the observations. Because of the availability of macroseismic observations only, we transformed the more sensitive ground shaking parameters of the advanced scenarios into intensity values with the awareness of the low resolution of the latter parameter as ground shaking indicator. Notwithstanding the uncertainties of the conversion relationships and the moderate magnitude (M_L = 5.2) of the event, the finite fault effects could have contributed to the anisotropic intensity distribution of the November 24, 2004 Salò earthquake.
In the framework of the recent improvement of knowledge about sources [DISS, 2006] and conversion relationships [Faccioli and Cauzzi, 2005], the use of synthetic simulations could contribute in the generation of realistic damage scenarios: indeed, even the differences between observed and estimated intensities (I_{MCS}-I_{est}) are less than those calculated by an isotropic attenuation relation (e.g. the mean of differences calculated with Grandori et al. [1991] is equal to –0.6 ± 0.8). Moreover, for practical use for the Civil Protection, synthetic simulations can contribute to identify areas, often not coincident with the epicentral ones, where increments of damage could occur (see, for instance, the case of April 11, 2003, Novi Ligure event M_W 4.9 [Podestà et al., 2006]).

Acknowledgements: The research was supported by DPC-INGV 2004-2006 convention (S3 Project)

5. REFERENCES

Anderson, J.G., Hough, S. (1984), A model for the shape of Fourier amplitude spectrum of acceleration at high frequencies , *Bull. Seism. Soc. Am.*, **74**, 1969-1994.

Augliera, P., D'Alema, E., Marzorati, S., Massa, M., De Gori, P., Marchetti, A., Cimini, G., Colasanti, G., Chiarabba, C., Vallocchia, M. (2006). Data set Garda 2004, INGV, only CD-ROM.

Bard (1998). SERINA: Seismic Risk and Integrated Seismological, Geotechnical and Structural Approaches. *ITSAK, European Commission*, Directorate General for Science and Development.

Bardet, J.P., IchiiI, K., Lin, C.H. (2000). *EERA A Computer Program for Equivalent-linear Earthquake site Response Analyses of Layered Soil Deposits*. Univ. of Southern California Department of Civil Engineering

Bernard, P., Madariaga, R. (1984). A new asymptotic method for the modeling of near field accelerograms, *Bull. Seism. Soc. Am.*, **74**, 539-558.

Bernardini, A., (a cura di) (2000). *La vulnerabilità degli edifice: valutazione a scala nazionale della vulnerabilità sismica degli edifici ordinaiy*. CNR-GNDT, Roma, 175 pp. + CDROM

Boore, D.(2003). Simulation of ground motion using the stochastic method, *Pure.Appl.Geophys.*, **160**, 635-676.

Boschi, E., Guidoboni, E., Ferrari, G., Mariotti, D., Valensise, G., Gasperini, P. (2000). Catalogue of Strong Italian Earthquakes, 461 b.C. to 1997, *Annali di Geofisica*, **43**, 609-868.

Bossu, R., Scotti, O., Cotton, F., Cushing, M., Levret, A. (2000). Determination of geomechanical site effects in France from macroseismic intensities and reliability of ,acroseismic magnitude of historical events, Tectonophysics **324**, 81-110.

D'Agostino, N., Cheloni, D., Mantenuto, S., Selvaggi, G., Nichelini, A., Zuliani, D. (2005). Strain accumulation in the southern Alps (NE Italy) and deformation at the northeastern boundary of Adria observed by CGPS measurements, *Geophys. Res. Let*., **32**, L19306, 10.1029/2005GL024266.

DISS Working Group (2006). Database of Individual Seismogenic Sources (DISS), Version 3: A compilation of potential sources for earthquakes larger than M 5.5 in Italy and surrounding areas. *http://www.ingv.it/DISS/,* Istituto Nazionale di Geofisica e Vulcanologia.

Doglioni C., Bosellini A.(1987) Eoalpine and Mesoalpine tectonics in the Southern Alps.*Geol.Rund*.,**76**,735-754.

Faccioli, E., Cauzzi, C. (2005). An attempt at improving felt intensity assessment of historical earthquakes by means of instrumentally based correlations. *Proceedings of Luis Esteva Symposium - Earthquake Engineering Challenges and Trends* - Mexico City, September 12, CD-ROM

Galadini, F., Galli, P., Cittadini, A., Giaccio, B. (2001). Late Quaternary fault movements in the Mt. Baldo-Lessini Mts. Sector of the Southalpine area (northern Italy), *Netherlands J. of Geosciences*, **80**, 187-208.

Grandori, G., Drei, A., Perotti, F., Tagliani , A. (1991). Macroseismic intensity versus epicentral distance: the case of central Italy. *Tectonophysics,* **193**, 165-171.

Guidoboni, E., Comastri, A. (2005). *Catalogue of earthquakes and tsunamis in the Mediterranean area from the 11th to the 15th century*, Istituto Nazionale di Geofisica e Vulcanologia.

INGV-Centro Nazionale Terremoti (2006). Seismic Bulletin. http://www.ingv.it/~roma/reti/rms/bollettino

ISTAT (1991). *13° ensimento generale della popolazione. Dati sulle caratteristiche strutturali della popolazione e delle abitazioni*. Roma

Kanamori ,H., Anderson, D. L. (1975). Theoretical basis of some empirical relations in seismology. *Bull. Seism. Soc. Am.*, **65**, 1,073-1,095.

Margottino, C., Molin, D., Narcisi, B., Serva, L. (1992). Intensity versus ground motion: a new approach using Italian data. *Engineering Geology,* **33**, 45-58.

Marzorati, S., Augliera, P., D'Alema, E., Bindi, D., Maistrello, M., Gassi A. (2004), The 2003 data set of seismic waveforms recorded in Lombardia and Veneto regions (Northern Italy): site selection and M_L scale calibration, ESC,XXIX General Assembly, September 12-17, 2004, Potsdam, Germany, p 60 (poster).

MEDNET (2006). MEDiterranean very broadband seismographic NETwork, INGV, *http://mednet.ingv.it/events/Welcome.html*.

Montone, P., Mariucci, M.T., Pondrell,i S., Amato, A. (2004). An improved stress map for Italy and surrounding regions (Central Mediterranean), *J. Geophys. Res*., **109**, 10.1029/2003jb002703.

Pacor, F., Cultrera, G., Mendez, A. and Cocco, M. (2005), Finite Fault Modeling of Strong Motion Using a Hybrid Deterministic-Stochastic Approach, *Bull. Seism. Soc. Am.*, **95**, 225-240.

Podestà, S., Resemini, S., Bindi, D., Spallarossa, D., Pacor, F. (2006). Spatial damage distribution and seismological aspects of the 11 April 2003 Novi Ligure (North Western Italy) M_W=4.9 earthquake. 1st ECEES, 2-8 september, Geneva, Switerland.

QUEST (QUick Earthquake Survey Team) (2005). Rilievo macrosismico del terremoto del Garda del 24 novembre 2004, *Ingegneria Sismica*, Anno XXII - N.2, 44-59.

Rebez, A. Slejko, D. (2004) Relazioni di conversione fra a_{max} e intensità, *Int. Report OGS-17/04/OGA-8*, 8pp.

Regione Lombardia e CNR (1996). *Determinazione del rischio sismico a fini urbanistici in Lombardia*.

Slejko, D., Carulli, G.B., Nicolich, R., Rebez, A., Zanferrari, A., Cavallin, A., Dogliosi, C., Carraio, F., Castaldini, D., Iliceto, V., Semenza, E., Zanolla, C. (1989). Seismotectonic of the eastern Southern-Alps: a review. *Boll. Geof. Appl*., **31**, 109-136.

SSN (2005), Dati accelerometrici prodotti dalla RAN (Rete accelerometrica Nazionale), Dip.Prot.Civ.-Ufficio Servizio Sismico Nazionale – Servizio Sistemi di Monitoraggio.

Spudich, P., Frazer, L.N. (1984) Use of ray theory to calculate high frequency radiation from earthquake sources having spatially variable rupture velocity and stress drop, *Bull. Seism. Soc. Am.*, **74**, 2061-2082.

Wells, D.L., Coppersmith, K.J. (1994). New Empirical Relationships among Magnitude, Rupture Length, Rupture Width, Rupture Area, and Surface Displacement, *Bull. Seism. Soc. Am.* **84**, 974-1002.

Zanferrari A., Bollettinari G., Carotene L., Carton A., Carulli G.B., Castaldini D., Cavallin A., Panizza M., Pellegrini G.B., Pianetti F., Sauro U. (1982). Evoluzione neotettonica dell'Italia nord-orientale. Mem. *Scienze Geologiche*, **35**, 355-376.